Quaternary Research (2019), **91**, 367–382.

doi:10.1017/qua.2018.58

Tropical Rainforest Dynamics and Palaeoclimate Implications since the late Pleistocene, Nilgiris, India

Priyanka Raja[a], Hema Achyuthan[a]*, Anjum Farooqui[b], Rengaswamy Ramesh[c], Pankaj Kumar[d], Sundeep Chopra[d]

[a]Department of Geology, Anna University, Chennai, India
[b]Birbal Sahni Institute of Palaeosciences, Lucknow, India
[c]School of Earth and Planetary Sciences, National Institute of Science Education and Research, Odisha, India
[d]Inter-University Accelerator Centre, New Delhi, India

(Received June 9, 2017; Accepted May 17, 2018)

Abstract

A multiproxy study involving sedimentology, palynology, radiocarbon dating, stable isotopes, and geochemistry was carried out on the Parsons Valley Lake deposit, Nilgiris, India, to determine palaeoclimatic fluctuations and their possible impact on vegetation since the late Pleistocene. The 72-cm-deep sediment core that was retrieved reveals five distinct palaeoclimatic phases: (1) Warm and humid conditions with a high lake stand before the last glacial maximum (LGM; ~29,800 cal yr BP), subsequently changing to a relatively cool and dry phase during the LGM. (2) Considerable dry conditions and lower precipitation occurred between ~16,300 and 9500 cal yr BP. During this period, the vegetation shrank and perhaps was confined to moister pockets or was a riparian forest cover. (3) An outbreak in the shift of monsoonal precipitation was witnessed in the beginning of the mid-Holocene, around 8400 cal yr BP, implying alteration in the shift toward warm and humid conditions, resulting in relatively high pollen abundance for evergreen taxa. (4) This phase exhibits a shift to heavier $\delta^{13}C$ values around ~1850 cal yr BP, with an emergence of moist deciduous plants pointing to drier conditions. (5) Human activities contributed to the exceedingly high percentage of *Acacia* and *Pinus* pollen during the Little Ice Age.

Keywords: LGM; Holocene; AMS radiocarbon dating; $\delta^{13}C$; Palynology; Nilgiris; CHNS; Palaeoclimate

INTRODUCTION

Tropical rainforests constitute a luxuriant equatorial biome with an extremely diverse array of vegetation and rich endemism. These distinctive rainforests are at present found mainly on detached fragments of Gondwanaland, a supercontinent during the Palaeozoic and early Mesozoic eras, excluding Southeast Asia (Corlett and Primack, 2006). The Western Ghats (WG) in peninsular India preserve a sizeable relic of these tropical evergreen rainforests, a product of millions of years of evolution (Prasad et al., 2009; Farooqui et al., 2010, 2014) that have been a centre of alpha diversity (Ghate et al., 1998; Myers et al., 2000; Bossuyt et al., 2004; Prasad et al., 2009). The WG, recognized as a UNESCO World Heritage Site and one of the eight "hottest biodiversity hot-spots" (Myers et al., 2000), comprise a continuous mountain range that runs about 1600 km north–south along the western coastline of India (Thomas and Palmer, 2007), sheltering 12 national parks and 44 wildlife sanctuaries. The WG include 2600 (75%) out of 3500 total plant species in the subcontinent, of which 1180 species out of 1300 (85%) show endemism (Blasco, 1971).

In the southern part of the WG, a unique kind of vegetation called the shola forest–grassland complex preserves a rich extant storehouse of endemic biodiversity. The word *shola* is derived from the Tamil word *cõlai*, meaning "thick vegetation canopy." The most typical shola occurs on the hilltops and plateaus of the Nilgiris at altitudes above 1800 m asl (Kumaran et al., 2008) and consists of undulating montane grasslands contiguous with stunted patches of tropical evergreen forest. The vast root systems of the shola help to retain runoff and prevent soil erosion, and therefore play an important role in supplying the headwaters of rivers and maintaining soil moisture (Swarupanandan et al., 1998). The shola complex falls within the Nilgiri Biosphere Reserve and is of ecological importance, providing a highly distinctive and extensive spectrum of habitats. The Nilgiri biome harbours 208 (55%) endemic plant species out of 365 species (Blasco, 1971), of which many are rare, endangered, or at the

*Corresponding author at: Department of Geology, Anna University, Sardar Patel Road, Chennai, Tamil Nadu 600025, India. E-mail address: hachyuthan@yahoo.com;hachyuthan0@gmail.com (H. Achyuthan).

brink of extinction. Once widespread, the shola biome is dwindling as a result of natural changes and human activities (Pramod et al., 1997). Climate change seriously jeopardizes the shola forests by affecting their microclimate and changing rainfall regimes. These alterations include increased variability in duration, magnitude, and timing of the monsoon rainfall.

Climate change has had a discernible impact on monsoon systems, consequently affecting the forest cover and vegetation. The Indian monsoon system, an important feature of global atmospheric circulation and the major seasonal climatic event across the Indian subcontinent is a manifestation of seasonal migration of the intertropical convergence zone (ITCZ) (Gadgil, 2003). The ITCZ, a subsystem of the global monsoon, is a deep, convective, cumulus cloud band near the equator where northeast and southeast trade winds converge. On seasonal time scales, the ITCZ migrates towards the warming hemisphere between average latitudes of 20°N in summer and 8°S in winter, accompanied by the southwest monsoon (onset phase/summer monsoon) and the northeast monsoon (retreat phase/winter monsoon), respectively, over the Indian landmass. The Nilgiris district receives rainfall from both monsoons (Schneider et al., 2014) following the seasonal march of the sun and maximum surface heating (Gadgil, 2003). The mean latitudinal position of the ITCZ and the intensity of convective activity control the onset, strength, duration, variability, and termination of the monsoons (Fleitmann et al., 2007). Variation in the mean latitudinal position of the ITCZ affects the tropical climate on a variety of temporal scales, ranging from annual to millennial. On longer time scales, palaeoclimate records demonstrate that the shift in mean latitudinal position of the ITCZ was similar, moving towards the differentially warming hemisphere and accompanied by significant changes in the hydrological cycle.

The tropical rainforests of the WG, particularly those of the shola, which receive incessant rains from both monsoons, are influenced by effects of variability in rainfall regime over longer time scales that could alter species richness. Annual rainfall and its seasonality are major determinants of species richness and diversity (Davidar et al., 2007). The rainforests are more sensitive to great climatic diversity like drought (Meir et al., 2015), are not resistant to water deficits for an extended period, and change in response to anomalously lower, prolonged, or recurrent precipitation (Angeler and Allen, 2016) by favouring deciduous species. They are dynamic and undergo directional shifts in structure and composition over decades to millennia (Feeley et al., 2007; Allen et al., 2017). Thus, high-amplitude regional rainfall and seasonality gradients due to short-term weather patterns or long-term climate oscillations significantly affect the ecologically sensitive shola, as do regional and local drivers. In addition, present-day sizeable threats to the shola forests result from the combined effects of frost, fire, grazing, invasive species, clearance for agriculture, fragmentation, encroachment, and the prevention of regeneration by rapid soil erosion (Karunakaran et al., 1998; Jose, 2012). Above all, silviculture has transformed these biodiverse forests into commercially valuable plantations of exotic trees. Hence, the shola forests, which took several thousands of years to evolve into their present state, are changing and shrinking at an alarming rate, resulting in loss of habitat for many species. The floristic composition, representing an evergreen forest climax community (Champion, 1936), is not regenerating, so the biome is dying and is befittingly termed a "living fossil" community (Vishnu-Mittre and Gupta, 1968).

The pace at which the evergreen forests are declining needs to be monitored and evaluated. Reconstruction of past vegetation successions can provide insight into the relationship between changing climatic conditions over thousands of years and the rate and direction of the long-term vegetation changes (Overpeck, 1993). Palynological evidence reveals the changing patterns of vegetation on late Quaternary landscapes and provides ample witness (Jacobson and Grimm, 1986) to vegetational changes that are not only climatically controlled but also ecologically mediated by local events such as fire and other disturbances. The study of pollen in stratified lake sediments provides a means for tracing the history of plant communities (Moore et al., 1991).

In this paper, quantitative records of sediment textural data, pollen abundance, and $\delta^{13}C$ values are interpreted in a ^{14}C-dated lake sediment core spanning ~29,800 cal yr BP. This paper is an attempt to reconstruct the palaeo-vegetation and palaeoclimate of Parsons Valley Lake region in the Nilgiri Hills, in order to illustrate the influence of the climate system on the vegetation, so as to aid in predicting the effects of future climate change.

STUDY AREA

Parsons Valley Lake (11°23′15.69″N, 76°36′10.8″E) lies in the Udhagamandalam Taluk of the Nilgiris District, Tamil Nadu, amidst the shola forests. This freshwater lake lies about 7 km east of Mukurthi National Park in the eastward realm of the WG (Fig. 1). The lake basin, irregular in shape with several bifurcating arms, measures ~3.75 km in length and ~1.5 km at its widest, covering an area of 202 hectares with an average surface elevation of 2200 m asl.

The geologic sediment in the lake bed and around the catchment is black in colour, due to the accumulation of humus in the top layers of shola soils. The black soil of this higher elevated western region, classified as an Andisol by Caner and Bourgeon (2001), is highly acidic in nature, with pH ranging from 4.5 to 6 (Mathur et al., 1984). The shola's soil texture varies from clay to clay-loam and loam and contains high percentages of iron and alumina along with maximum soil moisture and soil temperature when compared with all other vegetative covers. The bedrock is composed of Precambrian metamorphic rocks, mainly charnockites (gneisses, charnockites, and crystalline schist) (Naqvi and Rogers, 1987; Vasanthy, 1988) belonging to the Archean continental landmass.

The climate is classified as tropical monsoon type (Amw) characterized by heavy rainfall and a short dry winter under Köppen climate classification. High elevation of this region results in low temperatures (minimum10.0°C, maximum 29.8°C), which are driven yet lower by the excessive

https://doi.org/10.1017/qua.2018.58 Published online by Cambridge University Press

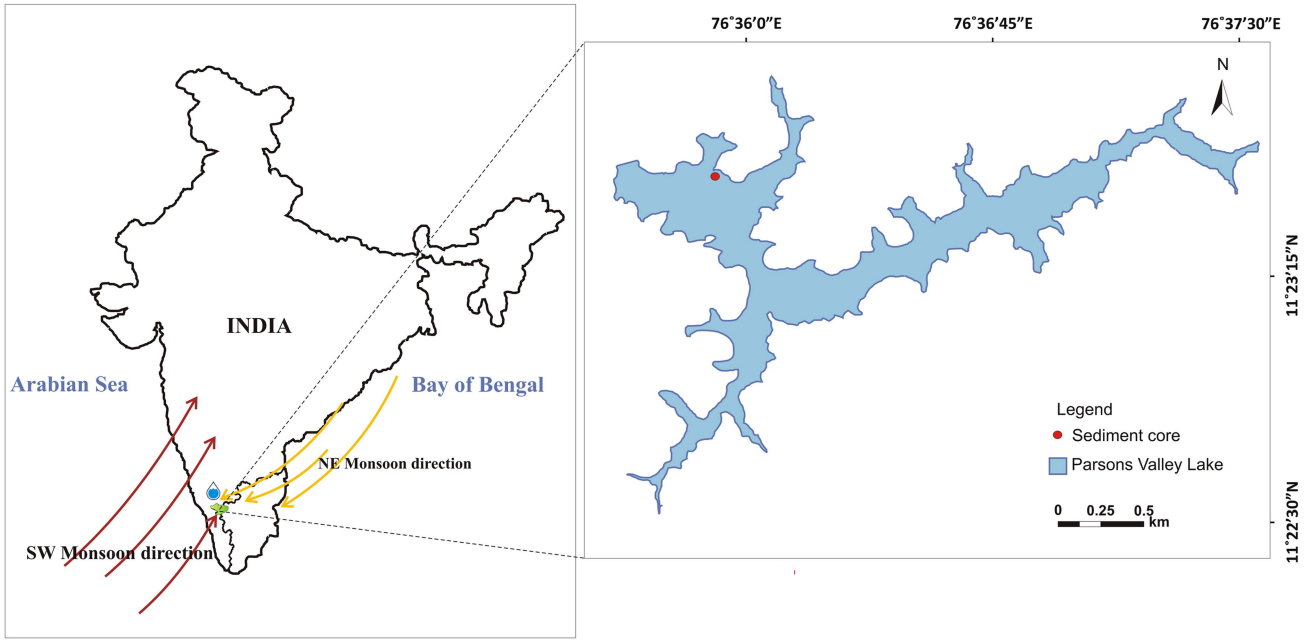

Figure 1. Location map of the Parson's Valley Lake in the Nilgiri Hills, Tamil Nadu, India.

atmospheric moisture content (humidity up to 90%; Suryaprakash, 1999) resulting from the thick vegetation cover. The total annual rainfall in this region ranges between 2500 and 5000 mm (Caner et al., 2007), and it receives its principal precipitation from the southwest monsoon and less intense northeast monsoon (derived from cooler air mass flowing off the Tibetan Plateau and adjacent regions in autumn, which picks up moisture from the Bay of Bengal and is important for precipitation in eastern parts of the Ghats; Kumaran et al., 2008), leading to luxuriant evergreen rainforests. The dominant overstory species in the shola belong to the members of Symplocaceae, Dipterocarpaceae, Lauraceae, Myrtaceae, Myrsinaceae, Oleaceae, and Rubiaceae, while understory species are dominated by Fabaceae, Asteraceae, and Acanthaceae. Monocotyledonous understory species are dominated by Cyperaceae, Poaceae, and Orchidaceae (Bunyan et al., 2012). Protected shola forests are in many cases surrounded by degraded forests and silviculture plantations of exotic *Acacia*, *Pinus*, and *Eucalyptus*. The natural vegetation of the region ranges from tropical evergreen to moist deciduous forests and swamps, all of which contributes to its high level of biodiversity. The humid west-facing valleys and gullies can maintain monsoonal rainforest under drier conditions, while deciduous elements will survive in drier sites such as ridgetops and eastern slopes.

MATERIALS AND METHODOLOGY

A 72-cm-long sediment core was retrieved manually from the Parsons Valley Lake (Fig. 1) by hammering acid-washed PVC pipe (75 mm [3 inch] diameter) into the lake bed at the selected location (a few meters from the lake margin at <1.5 m water depth, located using a Garmin III global positioning system). The lithology of the sediment core was described using a Munsell colour chart (Fig. 2), and measures of sediment texture and grain size distribution, including roundness and sorting, were collected. The sediment core was subsampled at 2 cm intervals, and each sample was sealed in a ziplock polyethylene bag, labelled, and preserved for further analysis. Samples for sediment and geochemical analyses were oven-dried at 40°C, and eight organic-rich sediment samples were radiocarbon-dated using accelerator mass spectrometry (AMS) at the Inter University Accelerator Center (IUAC), New Delhi (Table 1). The dried sediment samples were pretreated using the ABA (acid–base–acid) protocol after careful removal of plant microfossils either by wet flotation or manual extraction under a microscope. Sediment samples were placed in centrifuge tubes, immersed in 0.5 M HCl, and retained for heating and shaking at 65°C and 750 rpm for about 3 h to remove contaminant carbonates. After repeated washings with ultrapure water and centrifugation, the samples were brought to neutral pH. They were further treated with 0.1 M NaOH to remove humic and fulvic acids by heating and shaking at 65°C and at 750 rpm for about 3 h. After repeated washings and centrifuging, the pH-neutral sample was again treated with 0.5 M HCl to remove dissolved atmospheric carbon dioxide that might have been absorbed during the base wash. Finally, the sample was neutralized by repeated washing and freeze-dried for graphitization. Automated graphitization equipment was used for combustion and graphitization purposes (Wacker et al., 2010). Graphitized samples were measured using the AMS facility based on 500 kV tandem ion accelerator at IUAC, New Delhi (Kumar et al., 2015). An oxalic acid II sample from NIST (SRM 4990C) was used as a standard, and phthalic anhydride from Sigma-Aldrich (product no. 320064) was used as a blank for background correction. The radiocarbon dates were then corrected to the actual $\delta^{13}C$ values of the samples.

Twenty-one sediment samples were analysed for $\delta^{13}C$ values at the Physical Research Laboratory, Ahmedabad.

https://doi.org/10.1017/qua.2018.58 Published online by Cambridge University Press

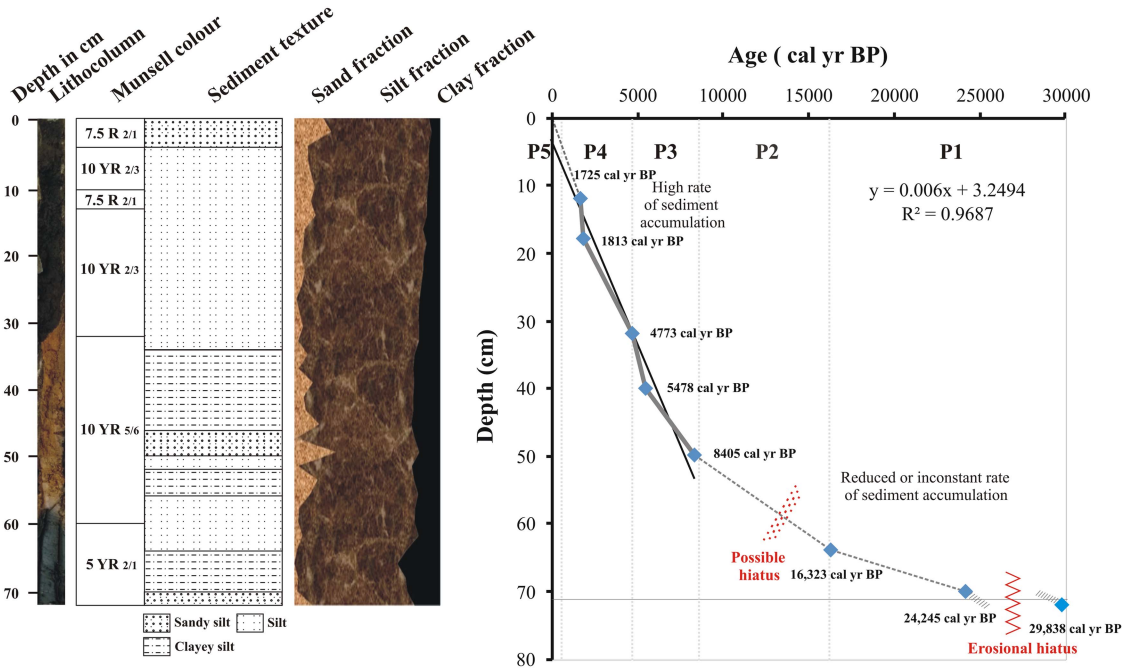

Figure 2. Sediment core lithologic units with depth vs radiocarbon ages.

Table 1. Radiocarbon ages of the lake sediments dated.

IUAC ID[a]	Sample ID	Depth (cm)	Radiocarbon age BP ± error	$\delta^{13}C$	Calibrated age range (2 sigma)	Midpoint calibrated age (cal yr BP)	Sedimentation rate (cm/yr)
16C356	PV 6	10–12	1811 ± 59	− 13.84	1876–1573	1725	0.0070
16C370	PV 9	16–18	1913 ± 58	− 16.90	1910–1716	1813	0.0033
16C358	PV 16	30–32	4244 ± 64	− 16.50	4965–4581	4773	0.0029
16C326	PV 20	38–40	4746 ± 92	− 15.29	5658–5298	5478	0.0015
16C328	PV 25	48–50	7626 ± 86	− 16.97	8595–8214	8405	0.0012
16C361 R	PV 32	62–64	13,512 ± 177	− 14.22	16860–15786	16,323	0.0009
16C362 R	PV 35	68–70	20,067 ± 801	− 14.90	26013–22476	24,245	0.0002
16C372	PV 36	70–72	25,613 ± 288	− 17.60	30595–29081	29,838	0.0001

[a]IUAC, Inter University Accelerator Center (IUAC), New Delhi.

Sand, silt, and clay percentages of the sediments were measured using Krumbein and Pettijohn's (1938) standard pipetting methods. Organic matter (OM) and carbonate content were measured using a loss-on-ignition method following Dean (1974); the sediment moisture was first removed by oven-drying at 50°C, followed by further heating of known weights of the samples at 550°C (for organic carbon) and 950°C (for carbonate). Carbon:nitrogen (C/N) ratios were determined using a Thermo Fisher Scientific FLASH 2000 CHNS-O organic elemental analyzer at the Department of Geology, Anna University, Chennai. The analytical accuracy for the estimation of total nitrogen and total organic carbon (TOC) is ±0.5%.

For palynological analyses, 10 g of each sample was first treated with 10% KOH and passed through a 150 mesh sieve (>106 µm). The filtrate was allowed to settle overnight, and the supernatant was discarded. The residue was acetolysed following Erdtman (1943) and subsequently filtered through a 650 mesh sieve (>10 µm). The residual matter containing the pollen and spores was mounted on glass slides using glycerine jelly and studied under a high-power light microscope (Olympus BX-51). The palynological spectra represent relative percentages of total counts (250–300) of pollen grains and spores. The total count (sum) excludes Poaceae/Cyperaceae (ubiquitous taxa) and algal and fungal spores and pteridophytic spores, as these taxa are disproportionately abundant, which may obscure vegetation interpretations (Cole et al., 2015). The recovered pollen grains were categorized as arboreals, nonarboreals, and aquatics, which are arranged accordingly in the same order in the pollen spectrum. Their relative percentages were calculated against the pollen sum. The pollen diagram and the cluster analysis (CONISS) were constructed using Tilia v. 1.7.16 (Grimm, 2011). The cluster analysis allowed us to infer the palynological phases by identifying homogenous segments of taxa (Table 2). The distribution of the recorded floristic types to relative mean precipitation and total number of dry months in

https://doi.org/10.1017/qua.2018.58 Published online by Cambridge University Press

Table 2. Palaeo-vegetation and its implication for climate change.

Palynozone	Depth (cm)	Time frame	Vegetation	Climate implication
I	72	29,800 cal yr BP	Characterized by the complete dominance of evergreen shola–semi-evergreen rainforest community	Warm and humid climate
	66–70	24,250–18,964 cal yr BP	Inception of temperate taxa Expansion of grassland.	Persistent cool and dry climate
II	64–52	16,300–9500 cal yr BP	A band of moist deciduous forests surround evergreen forests Expansion of grassland	Warm and less humid climate
III	50–34	8405–4949 cal yr BP	Dominance of evergreen shola vegetation with discontinuous stretches of tropical seasonal forests Decline in grasses	Warm and humid climate
IV	32–6	4773 cal yr BP	Evergreen shola forest vegetation	Increasingly warm and humid climate
	30–6	4350–862 cal yr BP	High seasonality Evergreen–semi-evergreen–moist deciduous Heterogeneous vegetation.	Decreasingly warm and humid climate
V	4–2	575–287 cal yr BP	Low species diversity Decline in rainforest elements	Cool and dry climate

the WG has been furnished in Supplementary Tables 1 and 2 to track the compositional shifts.

RESULTS

Lake sediment lithology

The stratified lake sediment core is divided into six lithologic units based on variations in both colour and texture (Fig. 2). Unit I (59.5–72cm) consists of very fine, blackish-grey clay deposits over a single layer of brownish-black clay (72 cm; 5 YR 2/1) (Fig. 2). Unit I is overlain by yellowish-brown sediments (10 YR 5/6), composed of alternate laminations of clayey silt and silt with one layer of sandy silt texture that occurs between 48 and 50 cm (unit II, 32–59.5 cm). Lithologic unit III (12.5–32 cm) is silty, brownish black in colour (10 YR 2/3), and poorly sorted. Lithologic unit IV (10–12.5 cm) has a gradational contact with unit III and contains coarse red sand grains (7.5 R 2/1). Lithologic unit V (4–10 cm) is silt dominant and brownish black in colour (10 YR 2/3) due to organic carbon. This unit is overlain by a reddish-black layer (7.5R 2/1) containing sandy silt that is poorly sorted and rich in OM and decayed leaves (unit VI, 0–4 cm).

Chronology

Eight organic carbon–rich samples were radiocarbon-dated, and the ages range from ~29,838 cal yr BP at 72 cm to ~1725 cal yr BP at 18 to 12 cm depth (Fig. 2, Table 1). This suggests a nonlinear sedimentation rate from the late Pleistocene to the present, with the apparent rates varying from 0.00006 cm/yr (from 29,838 to 24,245 cal yr BP; 72–70 cm) to 0.003 cm/yr (from 1813 to 1725 cal yr BP) and sedimentation rates generally increasing through the sequence (Fig. 2). Interpolated ages based on the eight measurements will be used here; however, the apparent very low sedimentation rates below 32 cm may indicate erosional episodes on the basin floor.

Sediment texture

The silt fraction (76.5%) is higher than the clay and sand throughout the core (Fig. 3). The clay component ranges from 29.42% (66 cm depth) to 5.91% (4 cm depth), while the sand fraction ranges from 28.52% (50 cm depth) to 0% (66 cm depth). A distinct increase in sand content was observed at the 2–4 cm depth (~570 cal yr BP), 48–50 cm (~8400 cal yr BP), and 52–54 cm (~10,650 cal yr BP).

OM, TOC, $CaCO_3$, and C/N ratio

The OM content in the sediment core increases abruptly from values averaging about 15% below 32 cm to values ranging between 28% and 34% above. The TOC content shows a similar shift from values less than 4% below 30 cm to values greater than 6% above ranging from 1.14% (depth 70 cm, corresponding to ~24,250 cal yr BP) to 7.71% (depth 18 cm, corresponding to ~1850 cal yr BP (Fig. 4). $CaCO_3$ exhibits a slight increase above 32 cm and is at its maximum value around ~290 cal yr BP (2 cm depth). C/N ratios fluctuate, especially in the top 30 cm of the core, but show a general tendency to increase with time. Average values are about 13 below 56 cm, and 17 above 30 cm.

Stable C isotope analyses

Lake sediment samples ($n = 21$) were analysed for $\delta^{13}C$, and the values range from −13.84% to −17.60‰ relative to the VPDB standard (Fig. 4). Around ~29,800 cal yr BP, a reasonably depleted $\delta^{13}C$ value of −17.60‰ is observed, which then

https://doi.org/10.1017/qua.2018.58 Published online by Cambridge University Press

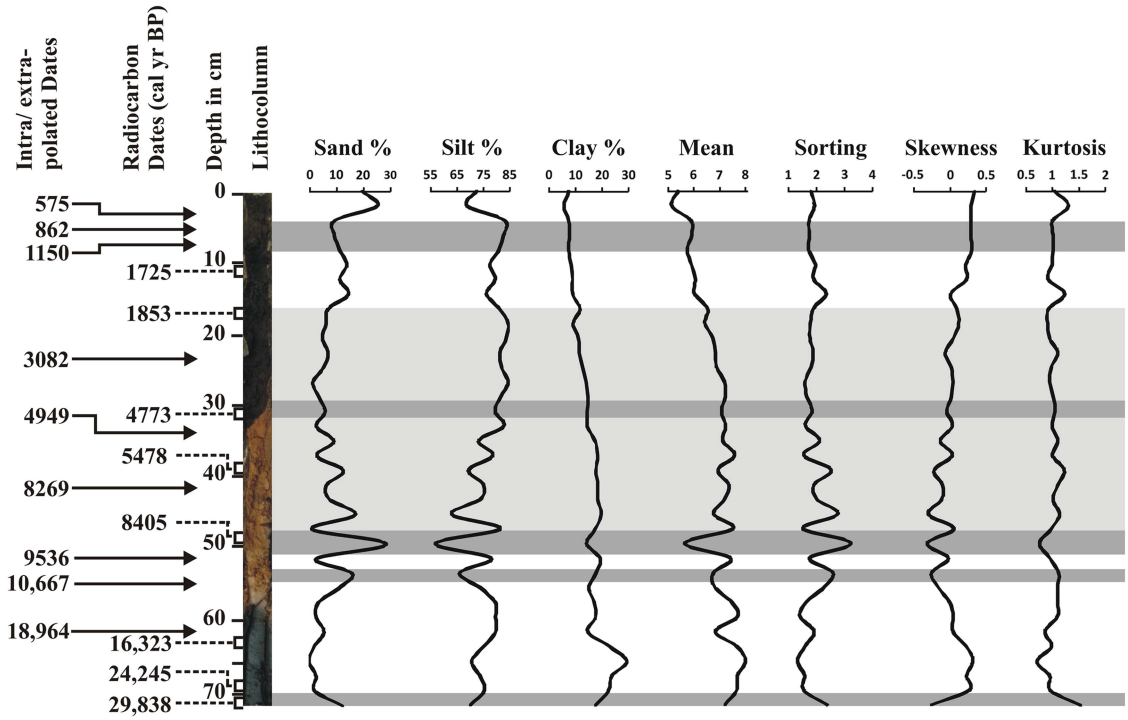

Figure 3. Down-core variations in sand, silt, and clay content; mean; sorting; skewness; and kurtosis. Intra/extrapolated dates refer to the estimation of age within/beyond the range of two known calibrated ages.

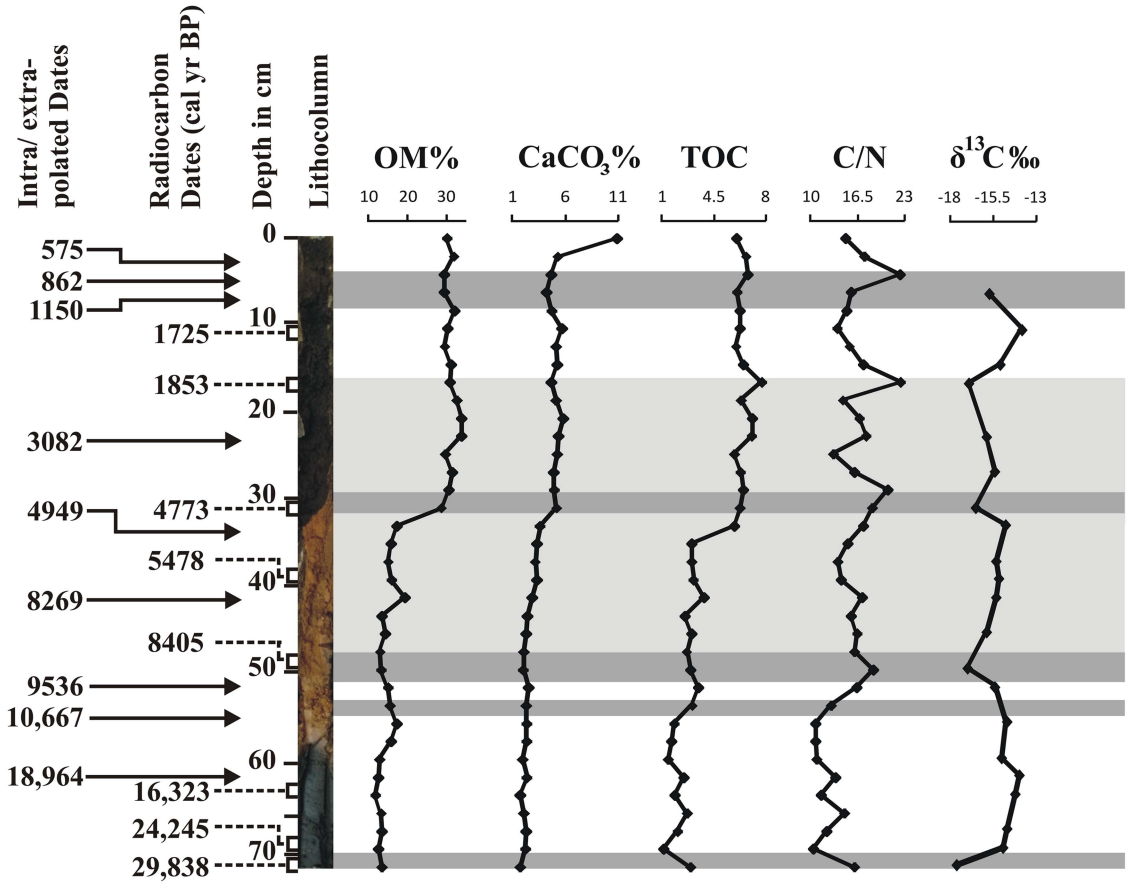

Figure 4. Down-core variations in organic matter (OM), $CaCO_3$, total organic carbon (TOC), C/N, and $\delta^{13}C$. Intra/extrapolated dates refer to the estimation of age within/beyond the range of two known calibrated ages.

https://doi.org/10.1017/qua.2018.58 Published online by Cambridge University Press

increases to −14.0‰ by ~15,200 cal yr BP. This enriched zone between ~24,200 to 11,800 cal yr BP indicates a mixture of C_4 and C_3 vegetation, followed by a declining trend between ~8400 to 4770 cal yr BP (−17.0 to −16.5 ‰). From ~4770 cal yr BP to the present represents a period of fluctuations containing more-negative $\delta^{13}C$ values, with an outlier of −13.84‰ at about ~1720 cal yr BP suggesting C_4 dominance. Overall, the values fluctuate around a mean of −15.4‰ in the core. An overall upward increase of nearly 3.8‰ in the $\delta^{13}C$ values reflects a significant change in the vegetation cover around the lake.

Palynology

Each of the sediment samples analysed revealed excellent preservation of pollen (Supplementary Fig. 1) and yielded a sufficient amount. The pollen sum of arboreal pollen (AP) and nonarboreal pollen (NAP) grains varied from 227 to 280, excluding Poaceae/Cyperaceae, algal and fungal spores, and pteridophytic spores. To delineate and to better understand the effect of climate change and sequential vegetation succession, we identified five distinct climatic phases on the basis of representation of prominent arboreal and nonarboreal species recovered, cluster analysis (CONISS), and other multiproxy data that are furnished separately (Supplementary Figs. 2 and 3).

Palynophase I (72–66 cm)

This pollen zone, with two radiocarbon dates of 29,800 and 24,250 cal yr BP, encompasses the temporal range of ~29,800 to 19,000 cal yr BP and is characterized by being completely dominated by an evergreen–semi-evergreen rainforest community. The total arboreal pollen (AP), constituting 81.3% of the total vegetation, is characterized by much higher values of *Myristica* (26.2%), followed only at the base by *Goniothalamus* (13.5%), Annonaceae (12%), *Rhododendron* (10%), *Hopea* (8.2%), *Hypericum* (7.2%), *Psychotria* (6.2%), *Drypetes* (3.2%), *Semecarpus* (2.5%), Anacardiaceae (2.2%), *Taraktogenos macrocarpa* (2.7%), and *Knema* (1.7%) at moderate to high frequencies. Other tree taxa, including *Terminalia* (1.5%), *Clausena* (1.5%), *Bentinckia* (1.2%), *Mangifera indica* (1%), *Artocarpus* (1%), *Nothapodytes* (1%), *Vateria* (0.75%), *Alnus* (0.75%), *Syzygium* (0.5%), and *Garcinia talbotii* (0.5%) are recorded sporadically. Among nonarboreal taxa, Asteraceae (10%) are recorded in high frequencies, followed by *Strobilanthes* (3%) and *Impatiens* (1.75%). Ranunculaceae (0.23%) represent the aquatic flora. Compared with the total pollen count, the relative percentage of pollen for the ubiquitous taxa Poaceae (19.08%) is highest, followed by Cyperaceae (8.9%), pteridophytic spores (6.3%), and algal and fungal spores (2.8%). The AP/NAP ratio (7.5) is highest in this phase (Fig. 5).

Palynophase II (64–52 cm)

This pollen zone, with a single radiocarbon date of 16,300 cal yr BP, covers an interpolated time interval of ~16,300 to 9500 cal yr BP and also exhibits dominance by arboreals (77.5%), but with a significant increase in nonarboreals. This zone displays a considerable increase in the number of tree taxa in

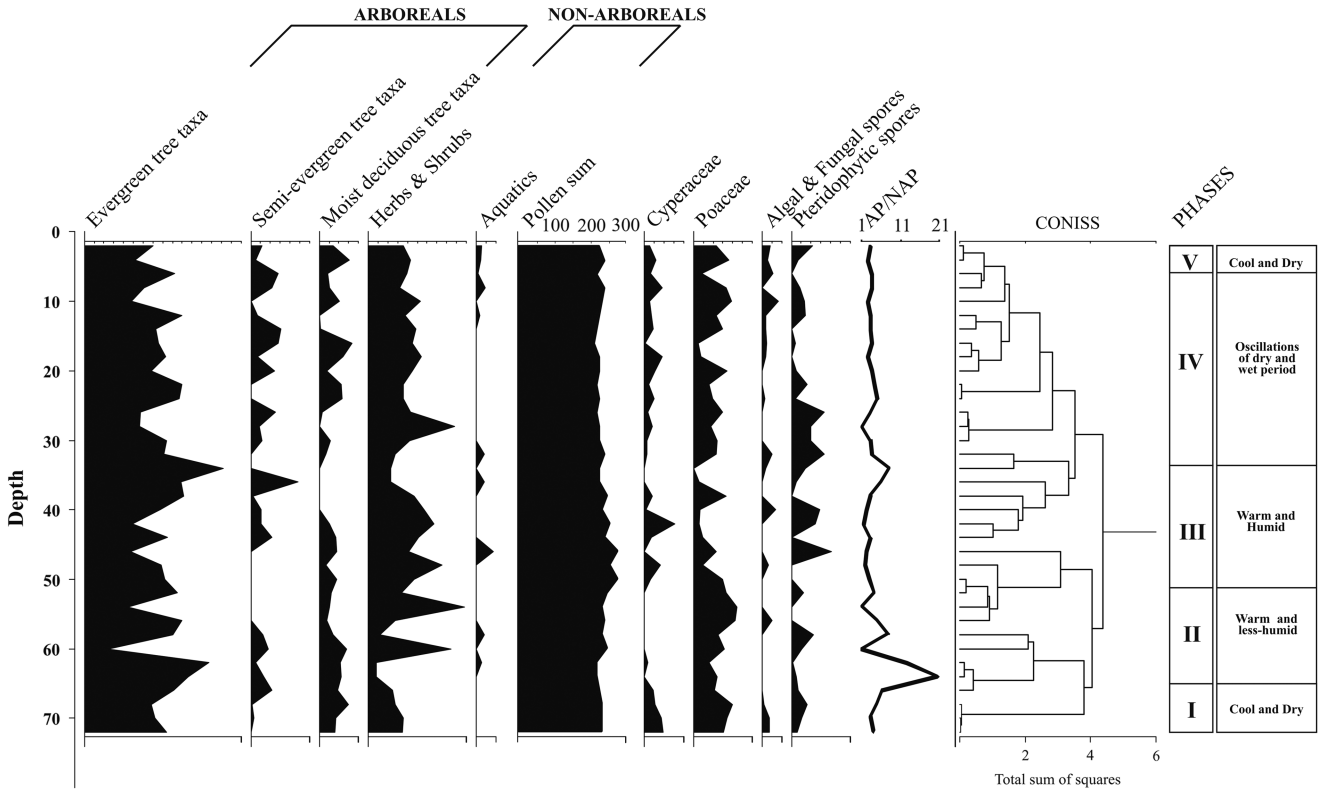

Figure 5. Palynological spectrum of functional types from Parsons Valley Lake core sediment, Nilgiris, India. AP, arboreal pollen; NAP, nonarboreal pollen.

https://doi.org/10.1017/qua.2018.58 Published online by Cambridge University Press

sporadic frequencies, interpreted as indicating high seasonality. The drought-resistant taxa Annonaceae (9.14%) maintains its constant presence in the zone. *Hopea* (8.71%), *Goniothalamus* (6.4%), *Myristica* (3.28%), *Macaranga peltata* (3.14%), *Isonandra* (3%), *Alnus* (2.57%), *Garcinia* (1.85%), *Walsura trifolia* (1.85%), *Knema attenuata* (1.71%), *Terminalia* (1.28%), *Croton* (1.28%), *Rhododendron* (1.14%), *Scolopia* (1.14%), *Artocarpus* (1%), Celastraceae (1%), and *Pajanelia longifolia* (1%) are recorded sporadically with moderate to low values. Enhanced intermittent values are recorded for *Vateria* (4.28%), *Garcinia talbotii* (1.14%), and *Humboldtia* sp. (0.71%) after a lapse, and the first appearance of *Gluta travancorica* (1.57%), *Vernonia* travancoria (1%), and *Dysoxylum malabaricum* (0.57%) in the upper part of this zone indicates the commencement of the Holocene. The nonarboreals show consistently high frequencies of *Impatiens* (6%) and Asteraceae (4.4%). *Myriophyllum* (0.57%) and Ranunculaceae (0.85%) represent the aquatic elements. Poaceae (15.02%) show consistently high frequencies followed by pteridophytic spores (3.59%). The marshy element, Cyperaceae (0.2%), along with algal and fungal spores (0.7%), is retrieved occasionally in very low frequencies. The AP/NAP ratio in this zone is 7.44.

Palynophase III (50–34 cm)

This pollen zone, with two ^{14}C dates of 8400 and 5480 cal yr BP and covering the time span of ~8,400 to 4950 cal yr BP, demonstrates further reduction in AP% (74.86%). Annonaceae (7.8%), *Hopea* (1.4%), *Myristica* (0.67%), and *Goniothalamus* (0.6%) have relatively reduced frequencies, in contrast to *Croton malabaricus* (3.3%) and *Artocarpus* (1.9%), which have enhanced values. *Artocarpus* (1.9%), *Eurya* (1.6%), *Poeciloneuron indicum* (1.3%), *Waltheria indica* (1.3%), Oleaceae (1.2%), *Kingiodendron pinnatum* (0.8%), *Otonephelium stipulaceum* (0.8%), Caesalpinaceae (0.8%), and *Reinwardtiodendron* (0.7%) are new entrants, with increased values recorded for them and for *Taraktogenos macrocarpa* (2.4%), *Aglaia* (2.3%), Tiliaceae (2.3%), *Waltheria indica* (1.3%), *Garcinia talbotii* (1.22%), Celastraceae (1%), *Vateria indica* (0.89%), and *Alnus* (0.8%), indicating a thick evergreen–semi-evergreen rainforest cover in the vicinity. Among the herbaceous elements, Asteraceae (6.5%) shows high frequencies followed by *Impatiens* (3.55%), *Cannabis sativa* (1.5%), Apiaceae (1.33%), and *Chlorophyton* (0.55%). The aquatic elements *Pistia stratiotes* (1.1%) and Ranunculaceae (0.9%) emerge sporadically. The considerably reduced value for Poaceae (5.74%) indicates its growth has been restricted by a dense rainforest community. Increase in the wetland taxa Cyperaceae (3.11%), pteridophytic spores (5.9%), and algal and fungal spores (1.3%) suggests a wetter climate. The AP/NAP ratio is 3.46.

Palynophase IV (32–6 cm)

This pollen zone, represented by three radiocarbon dates of 4700, 1850, and 1720 cal yr BP and with a time bracket from ~4770 to 860 cal yr BP, documents considerably increased numbers of both arboreal (64) and nonarboreal taxa (13) when compared with all other pollen zones. The AP constitutes 76.7% of the total pollen count. About 11% is Annonaceae (11%), followed by *Decussocarpus* (6.4%), Tiliaceae (5.57%), *Myristica* (5%), *Rhododendron* (4.2%), *Ilex* (3%), *Artocarpus* (3%), *Hopea* (2%), *Elaeocarpus* (2%), *Croton malabaricus* (2%), *Alnus* (1.9%), *Eurya japonica* (1.7%), *Otonephelium stipulaceum* (1.7%), *Poeciloneuron indicum* (1. 5%), Celastraceae (1.42%), *Taraktogenos macrocarpa* (1.4%), *Acacia* (1.3%), Rubiaceae (1.3%), *Isonandra lanceolata* (1.3%), *Mitracarpus verticillatus* (1.2%), *Memecylon talbotianum* (1.2%), *Vernonia travancoria* (1.1%), *Hypericum* (1%), *Goniothalamus* (1%), *Diospyros* (1%), and Flacourtiaceae (1%). The NAP assemblage is composed of *Impatiens* (7%), Asteraceae (7%), Apiaceae (5.8%), *Chlorophyton* (2.8%), *Cannabis sativa* (1.6%), *Xanthium* (1%), *Strobilanthes* (0.5%), *Artemisia* (0.4%), and Brassicaceae (0.4%). Ranunculaceae (1%) is the lone, sporadically recorded aquatic element. Poaceae constitutes 13.2%, Cyperaceae 4.3%, pteridophytic spores 7.2%, and algal and fungal spores 2.3%. The AP/NAP ratio is 3.3.

Palynophase V (4–0 cm)

This pollen zone covers the temporal range from ~570 cal yr BP to the present and depicts considerable reduction in arboreal diversity. The total AP constitutes 73.7%, with a drastic decline in the number of arboreals. *Pinus* (14%), *Gluta travancorica* (5.5%), *Turpinia* (3.5%), *Reinwardtiodendron* (2.5%), *Baccaurea courtallensis* (2.5%), *Scolopia* (1.5%), and *Symplocos* (1%) have relatively increased values in this pollen zone. However, Annonaceae (5.5%), Rubiaceae (2%), *Syzygium* (1.5%), *Ixora* (1.5%), *Psychotria* (1.5%), Meliaceae (1%), and *Myristica malabarica* (1%) show a decline. *Ilex sulcata* (1.5%) appears for the first time. The advent of moist deciduous elements such as *Terminalia* (3.5%), *Canarium strictum* (2.5%), *Nothapodytes* (2%), and *Acacia* (2%), along with *Rhododendron* (4%), is seen, and these plants are identified in appreciable numbers. The NAP taxa also become less diverse in this zone, with *Impatiens* (5%), *Artemisia* (4%), Asteraceae (3.5%), Apiaceae (3%), *Strobilanthes* (1.5%), *Xanthium* (1.5%), and *Clerodendrum viscosum* (1.5%) recorded sporadically with high to moderate values. A spurt in aquatic vegetation is documented with high values for *Polygonum plebeium* (3.5%) together with Ranunculaceae (0.7%). Poaceae (17.1%), Cyperaceae (5%), pteridophytic spores (8.6%), and algal and fungal spores (4%) are marked by relatively increased values. The AP/NAP ratio is down to 2.8.

DISCUSSION

Based on the integration of our results, we have classified the core into five palaeoecological zones.

https://doi.org/10.1017/qua.2018.58 Published online by Cambridge University Press

Phase I: Climate and vegetation during the pre–last glacial maximum and last glacial maximum

The multiproxy evidence collectively delineates a prominent wet phase in the last glacial period at around ~29,800 cal yr BP (72 cm). The sediment exhibits a brownish-black (5 YR 2/1) colour, probably due to anoxic conditions during periods of stagnation, and has recorded a relatively enhanced sand flux and C/N values indicating greater terrestrial input. The sediments are very poorly sorted, very leptokurtic, and coarse skewed, which suggests hydrodynamic scour caused by high-energy water currents carrying larger clasts into the lake, with the finer sediments travelling to and accumulating in a deeper part of the lake. This phase also shows the most depleted $\delta^{13}C$ signature (–17.6‰), suggesting an abundance of C_3 vegetation interpreted to be related to high soil moisture (Rajagopalan et al., 1997) (Fig. 4). Thirteen out of 17 tree taxa recorded in this wet phase represent highly diverse evergreen to semi-evergreen rainforest vegetation. The moderate representation of a few emergent moist deciduous elements such as *Hypericum*, *Terminalia*, and *Rhododendron*, which increase at the time of the last glacial maximum (LGM), is possibly a pioneer response attesting to the gradual replacement of the widespread evergreens. The highest percentage of *Myristica malabarica* and *M. fatua* are recorded, suggesting swampy areas in the vicinity, which indicates heavy precipitation during this period (Supplementary Fig. 2, Supplementary Table 1). The presence of *Hopea*, *Vateria indica*, *Artocarpus*, *Garcinia talbotii*, *Taraktogenos*, and *Strobilanthes* pollen also indicates high rainfall during this period around ~29,800 cal yr BP, contemporaneous with northward displacement of the ITCZ (Peterson and Haug, 2006). Such a wet phase might have extended before 29,800 cal yr BP, but lack of data from our present study inhibits our inferences. In their work on peat samples in the Sandynallah region of the Nilgiris, Rajagopalan et al. (1997) suggested relatively moist conditions between 40,000 and 20,000 years BP in South India, affirming our results. However, this millennial-scale pulse of high precipitation is not observed in the wider region, suggesting a climatic response to local forcings in the Parsons Valley region. This contrasts with several palaeoclimate reconstructions showing a widespread arid phase at this time in low latitudes (Kristen et al., 2007; Tierney et al., 2008; Rusella et al., 2014; Dutt et al., 2015).

The subsequent sediment sample (70 cm) of radiocarbon age ~24,250 cal yr BP indicates an apparent erosional hiatus in the sequence, as it encompasses a measurable interval of geologic time (Mitchum, 1977).

During the Heinrich 2 event (~23,000 cal yr BP; Bard et al., 2000) and the global LGM, the climate of the Parsons Valley region was marked by a transition to a cool climate with an estimated temperature drop of 5°C (Farrera et al., 1999) induced by low solar forcings (Sirocko et al., 1993). This zone is associated with very slow sedimentation rates, with clay dominance (avg. 73%), particularly around 18,960 cal yr BP (interpolated age; depth 66 cm), and an absence of sand that indicates a significantly weaker monsoon (Cosford et al., 2010). This is corroborated by enriched $\delta^{13}C$ values. The pollen assemblage reveals heterogeneity, as both temperate and tropical trees were recorded. The expansion of *Rhododendron* and *Hypericum*, along with incursion of *Alnus*, suggests a cooler climate. Consistent high frequencies of Asteraceae (interpreted as being indicative of cooler, dry conditions), is attributed to a northeast monsoon domination during this period (Tiwari et al., 2006; Ansari and Vink 2007; Chabangborn et al., 2013). Although cool conditions persisted for a few millennia, the climate also became seasonally drier in the region and saw reduced precipitation overall, as indicated by high percentages of drought-resistant tree taxa like Meliaceae, *Terminalia*, and Annonaceae (Supplementary Fig. 2). However, the prevalence of such an intensified cool and dry spell did not affect the shola forests, which exhibit high water-retention capacity due to their microenvironment and its higher relative humidity. Furthermore, the cooler temperature would have decreased the evaporation rate (Yu et al., 2000) and increased the moisture availability in the Parsons Valley Lake, which is inferred from the blackish-grey colour of the sediments (5 YR 2/1; reduction of minerals) and sediment texture (clayey silt), indicating high lake stands for longer periods. Relating to the moisture availability, the overall AP% of this phase remained high (81.3%), indicating the abundance of less diverse populations with low seasonality (Barboni and Bonnefille, 2001) (Fig. 5).

The persistent cool and dry climatic conditions that prevailed in the South Asian region during the LGM are attributable to a strengthened northeast monsoon and weakened summer monsoon circulation corresponding to broad insolation minima and a southward-displaced ITCZ (Shin et al., 2003; Liu et al., 2005; Kristen et al., 2007; Fleitmann et al., 2011; Konecky et al., 2011; Rusella et al., 2014). Climate model (CCSM3) simulations and reconstructed palaeo-data for the Asian monsoon region indicate a weak LGM summer monsoon over most of the Indian Ocean subregion (Chabangborn et al., 2013), suggesting the prevalence of cool and dry conditions.

Phase II: Climate and vegetation during the latest Pleistocene and Pleistocene–Holocene transition

During the post-LGM period (~16,300 to 9500 cal yr BP), the variations in deposition of terrigenous silty sediments and their grain size distribution document large precipitation changes and fluctuating lake levels. This interval demonstrates a general shift towards a wet–dry tropical climate comprising episodes of intense, excessive summer monsoon years interrupted by infrequent monsoon failures, which led to repetitive episodes of desiccation and refilling of the lake. The low rates of sediment accumulation imply sediment hiatuses of erosive origin consistent with periods of stronger monsoons (Sadler, 1999; Servant-Vildary et al., 2001) or discontinuous sedimentation associated with intervals of dry conditions and reduced sediment supply (Zhang et al., 2014).

https://doi.org/10.1017/qua.2018.58 Published online by Cambridge University Press

The sediment texture, characterized by clayey silt, displays a yellowish-brown colour (10 YR 5/6), indicating oxidized conditions—a consequence of historically fluctuating lake levels. This period has a reduced AP% (from 81.3% to 77.5%), but with higher diversity compared with the preceding pollen zone, exhibiting 18 new entrants of largely evergreen rainforest taxa that occur in low frequencies, such as *Gluta travancorica*, *Meiogyne pannosa*, *Garcinia*, *Diospyros*, *Croton malabaricus*, *Humboldtia* sp., *Isonandra lanceolata*, and *Aglaia* in response to the stabilized temperatures. Reduced numbers of *Rhododendron*, *Hypericum*, and *Terminalia*, along with extremely low frequencies of *Myristica* and sedges, point to the termination of cool and waterlogged conditions. However, sporadic representation of a few moisture-loving plants like *Myriophyllum* and Ranunculaceae indicates occasional high lake stands despite the elevated temperature and strong insolation forcing, suggesting intermittent episodes of higher summer precipitation. During periods of reduced monsoonal activity with lowered effective rainfall, drought-intolerant vegetation shrank and perhaps took refuge around the moister pockets or as riparian forest cover, restricted to locales with edaphic conditions favourable to its sustenance, resulting in a consistent AP record. Most of the species recorded during phase I (*Semecarpus*, *Bentinckia condapanna*, *Hypericum*, *Drypetes*, Flacourtiaceae, *Myristica fatua*, and *Syzygium* sp.) show time-bracketed local extirpations, especially during the latter part of this phase, probably due to weakened regeneration capacity in the changing environment. A distinct, intense wet phase identified during the post-LGM warming phase at about ~10,650 cal yr BP indicates a climatic anomaly pattern of considerably stronger and active precipitation reflected in enhanced sand influx of a very poorly sorted, coarse skewed, and leptokurtic nature, with an elevated TOC value. In the present study, the sediment core is chiefly dominated by fine-grained silts and clays, which reflects sedimentation during perennial water inflows that commonly occur, so the coarse-grained clastic layers punctuating this silty matrix reflect the very highest energy wet environment (Priyanka et al., 2018). It is possible that the wet events indicated by a major shift in the magnitude of the sediment data in our record are associated with the commencement of the early Holocene intensification of summer monsoons, although our age control is insufficient to constrain their timing within a period of possible unconformity. A relatively high percentage of pollen of *Garcinia talbotii*, *Hopea ponga*, and *Humboldtia* sp., coupled with a decline in drought-resistant taxa like Annonaceae and incursion of *Chlorophyton*, *Vernonia travancoria*, *Impatiens*, and *Villebrunea integrifolia* interspersed among rainforest tree taxa, indicates rainforests of low diversity occurred in and around the periphery of the Parsons Valley Lake as a result of intense precipitation during the very early Holocene period when summer insolation was the highest (Roy and Singhvi, 2016).

The overall shift towards an ameliorated thermal regime during the last deglaciation period synchronises well with the African humid period (Holmes and Hoelzmann, 2017) and insolation-driven changes occurring around 16,000 yrs BP with the onset of the Bølling/Allerød warming (Claussen et al., 2017). Oscillating patterns of decadal- and centennial-scale variability of humid periods, punctuated by arid episodes, indicate an alternation of intermediate and shallow lake stands. Higher summer insolation in India with an increase in the Indian Ocean Sea Surface Temperature (SST) shifted the ITCZ to northern latitudes (Peterson and Haug, 2006; Yancheva et al., 2007; Roy and Singhvi, 2016), bringing in more summer precipitation during latest Pleistocene and Pleistocene–Holocene transition. However, uninterrupted insolation forcing in the high-montane tropical lake, with intermittent break periods of relatively lesser amounts of summer rainfall, would have probably caused drier spells and shallow lake stands. Consistent AP concentrations in the region are probably the result of local factors that maintained a continuous pollen record of more diverse evergreen landscape in the expansive riparian zones. In their work on land-cover response to climate change in the Nilgiris, Caner et al. (2007) demonstrate that, beaten by strong southwest monsoon winds in the western Nilgiris (where Parsons Valley lies), sholas expanded in sheltered valley sites, which led to slow but steady expansion of the forest cover since 18 ka BP. This alternating active and inactive monsoon phase in the Parsons Valley appears to have been interrupted by an intense intervening spell of torrential rains before 10,000 yrs BP. Higher lake levels (Bartlein et al., 2011) associated with temperature increases (Wang et al., 1999; Markgraf et al., 2007), intensified Indian summer monsoon (Deplazes et al., 2013), a weakened northeast monsoon (Wang et al., 1999), and C_3 vegetation dominance in Nilgiris (Sukumar et al., 1993) support the existence of wet conditions during this time period. The commencement of the early Holocene intensification around 10,650 cal yr BP, as marked by pluvial conditions, corroborates well with the summer insolation maximum (Sirocko et al., 1993; Overpeck et al., 1996) and advancement of the ITCZ more into northern latitudes (Kutzbach and Guetter, 1986; Liu et al., 2006; Roy and Singhvi, 2016).

Phase III: Climate and vegetation during the early to mid-Holocene and mid-Holocene

The early to mid-Holocene transition around ~8405 cal yr BP witnessed an outbreak in monsoonal precipitation indicated by the highest sand content (28.5%) in the core. This significant seasonal contrast in response to insolation forcing was brought about regional changes in the hydrologic cycle and global monsoons (Berger, 1978). Enriched C/N ratios and less positive $\delta^{13}C$ values suggest a period of dominant C_3 terrestrial input that further supports this wet event interpretation (Fig. 4). The presence of *Poeciloneuron indicum*, *Garcinia talbotii*, *Terminalia*, and *Hopea ponga*, coupled with re-established populations of Asteraceae and Cyperaceae, indicates a higher relative summer monsoon in the region as well as an active northeast monsoon, corroborating

https://doi.org/10.1017/qua.2018.58 Published online by Cambridge University Press

Table 3. Comparison of the observed Parsons Valley Lake $\delta^{13}C$ data with values taken from the literature for samples dated from the late Pleistocene to the present.

		Time frame					
		Late Holocene	Mid-Holocene	Early Holocene	Post-LGM[a]	LGM[a]	Pre-LGM[a]
		4.2 ka BP to present	8.2–4.2 ka BP	11.7–8.2 ka BP	19–11.7 ka BP	26.5–18 ka BP	
Reference	Area investigated	(Walker et al., 2012)	(Walker et al., 2012)	(Walker et al., 2009)		(Clark et al., 2009)	
Galy et al., 2008	Bengal Fan sediments from cores 117KL, 118KL, and 120KL	−21.52	−21.76	−20.48	−19.86	−18.8	*
Newnham et al., 2007	Kohuora crater, Auckland	−29.3	−31.2	*	−26.92	−24.3	−26.35
Andreev et al., 2002	Labaz Lake area sequences	−28.07	−27.11	−28.49	−28.01	−27.63	−29.05
Sinninghe Damsté et al., 2011	C_{31} *n*-alkane record, eastern equatorial Africa	−28.6	−29.2	−28.9	−25.1	−24.1	*
Hamdan and Brook, 2015	Eastern desert and Sinai of Egypt (residual organic matters)	−26.4	−23.82	−24.14	−23.7	−23.34	*
Caner et al., 2007	Soils of western region (Nil 16), Nilgiris	−16.58	*	*	*	−12.1	*
Rajagopalan et al., 1997	Sandynallah region of the Nilgiri Hills	−16.28	−15.8	−17.36	−16.26	−18.6	−18.85
Present study	Parsons Valley Lake, Nilgiris	−15.49	−15.49	−16.80	−14.48	−14.78	−17.60

[a]LGM, last glacial maximum. (*) = data not available.

Rajagopalan et al. (1997), who suggest excess soil moisture (more negative $\delta^{13}C$ values) in the Sandynallah basin, Nilgiris (Table 3).

During the mid-Holocene, frequent or prolonged breaks in the intensity of rainfall are depicted by fluctuating C/N and TOC trends that indicate short-term climatic variability with an overall subnormal performance of the summer monsoon. Clayey-silt sediments of an oxidised nature indicate decreasing sediment input as a result of variable rainfall and reduced length of the monsoon season in response to changing summer solar insolation in the Northern Hemisphere (Overpeck et al., 1996; Fleitmann et al., 2004; Wang et al., 2010) and a gradual decrease in summer monsoon (Roy and Singhvi, 2016). The average $\delta^{13}C$ value in this period ranges around −15.6‰, suggesting a shift towards C_4 grassland vegetation (Rajagopalan et al., 1997). This zone records a reduction in AP% corresponding to increased representation by nonarboreals. The increase in nonarboreals suggests an opening up of the forest related to a weakened summer monsoon, suggesting lakes with fluctuating margins. The pollen record indicates a dominance of rainforest vegetation interrupted by discontinuous stretches of seasonal tropical forests. There is a scattered presence of rainforest elements comprising members of Oleaceae and Dipterocarpaceae, *Goniothalamus*, *Meiogyne pannosa*, *Artocarpus*, *Eurya japonica*, *Isonandra lanceolata*, *Garcinia talbotii*, *Poecilo-neuron indicum*, *Kingiodendron pinnatum*, *Taraktogenos macrocarpa*, *Reinwardtiodendron*, *Aglaia*, *Myristica malabarica*, and *Prunus ceylanica*, which flourish in the WG in areas of high precipitation (2500–5000 mm/year), along with other low-diversity heterogeneous (semi-evergreen and deciduous) components such as *Alnus*, *Pajanelia*, *Mallotus*, *Hydnocarpus*, and *Croton malabaricus*, suggesting frequent long breaks with sparse rainfall during this overall warm period (Roy and Singhvi, 2016).

This prominent period, extending from ~8400 to 4950 cal yr BP, corresponds with the Holocene climate optimum (HCO) (Ruiz-Zapata et al., 2010). Similarities between $\delta^{13}C$ records from Parsons Valley Lake in Nilgiris, $\delta D_{leaf\ wax}$ records of Lake Tanganyika in East Africa (Tierney et al., 2008), speleothem records from Mawmluh Cave in East India (Dutt et al., 2015), bulk dry density records from Dahu Swamp in South China (Zhong et al., 2012), Ti% from the Cariaco basin in Venezuela (Peterson and Haug, 2006), and SST records from the northwestern Arabian Sea (Böll et al., 2015), along with a series of solar maxima (Usoskin et al., 2007), suggest a strengthened Holocene summer monsoon related to a northward shift in the ITCZ around the early–middle Holocene boundary (Koutavas and Lynch-Stieglitz, 2004; Schneider et al., 2014; Roy and Singhvi, 2016). Conversely, a gradual reduction in monsoon intensities occurred after the HCO, accompanied by a southward shift in the ITCZ driven primarily by orbitally induced changes in insolation at multidecadal and centennial time scales (Gupta et al., 2003; Koutavas and Lynch-Stieglitz, 2004; Fleitmann et al., 2007; Wanner et al., 2008; Konecky et al., 2011; Schneider et al., 2014; Dutt et al., 2015, Ramisch et al., 2016).

https://doi.org/10.1017/qua.2018.58 Published online by Cambridge University Press

Phase IV: Climate and vegetation during the mid- to late Holocene and late Holocene

The mid- to late Holocene transition period records multiple decadal- to centennial-scale wet events associated with a more northward shift of the ITCZ. An environmental threshold during this transition was identified around ~4770 cal yr BP with an abrupt increase in OM and an enhanced C/N ratio interpreted as greater terrestrial input. This is corroborated by a tendency towards a more negative $\delta^{13}C$ record (Thevenon et al., 2012). Generally, changes in rates of TOC burial in lakes or changes in redox conditions reflect major changes in terrestrial vegetation and climate (Plater et al., 2006). Hence, the increase of terrestrial OM (Fig. 4) can be related to the expansion of a C_3 vegetation landscape (Thevenon et al., 2012) resulting from abundant moisture availability. Enrichment in rainforest vegetation occurred, with an appreciable number of evergreen tree elements such as *Poeciloneuron indicum*, *Elaeocarpus*, *Taraktogenos macrocarpa*, *Artocarpus*, *Myristica malabarica*, and *Leptonychia moacurroides* becoming established in response to an ameliorated hydrothermal regime. This coincides with increased rainfall in Tatos basin, Mauritius, around 4750 cal yr BP (de Boer et al., 2014).

Conversely, during the late Holocene period from 4350 to 862 cal yr BP, relatively lower values of C/N and an increased fine terrigenous fraction reflect reduced erosive rainfall energy, corresponding with a decrease in the strength of the summer monsoon (Roy and Singhvi, 2016, Böll et al., 2015). In particular, a heavier $\delta^{13}C$ signature supported by elevated proportions of Poaceae pollen around ~1725 cal yr BP clearly indicates significant C_4 contribution in response to lower effective moisture. An increase in $CaCO_3$ content suggests stronger evaporative conditions and supports weakened monsoon activity. Two wet intervals indicated by less positive $\delta^{13}C$ values and higher C/N ratios that occurred around 1853 and 1150 cal yr BP correlate with frequent high-intensity El Niño southern oscillation (ENSO) events (Moy et al., 2002; Steinke et al., 2014; Roy and Singhvi, 2016) (Fig. 4).

Although the percentage of AP remains static, the number of species has increased drastically by 42% (64 tree taxa), which is related to high seasonality (Beuning et al., 2011). The expansion and diversification of the vegetation with incursions of temperate elements and most herbaceous taxa suggests increased rainfall seasonality. The sporadic occurrence of rainforest taxa such as *Gluta travancorica*, *Poeciloneuron indicum*, *Elaeocarpus*, and *Aglaia*, which grow in high-rainfall conditions, along with new entrants such as *Calophyllum apctalum*, *Baccaurea courtallensis*, *Nothapodytes foetida*, *Memecylon talbotianum*, *Decussocarpus*, *Rosa canina*, *Ixora* sp., *Thraulococcus erectus*, *Mimusops elengi*, *Turpinia malabarica*, and *Leptonychia moacurroides*, indicates a rainfall regime with a single long rainy season. Occasional high values of algal and fungal spores during this phase are significant, indicating occasional excess moisture conditions (Power et al., 2006). Deciduous taxa intrusions like *Acacia*, *Calliandra portoricensis*, and *Drypetes oblongifolia*, along with drought-resistant taxa belonging to the Annonaceae and Meliaceae, indicate a less effective monsoon. An increase in frequencies of taxa belonging to Apiaceae and Asteraceae with a well-developed marshy fringe around the lake indicates a winter high-rainfall regime (Supplementary Table 2). Thus, the region remained sufficiently moist, with the bulk of rainfall concentrated in the winter season, implying a continued lack of a long dry season and revealing weak and variable summer monsoons alternating with strengthened winter monsoons.

During the late Holocene, the mean position of ITCZ gradually relocated farther southward, influenced by insolation changes. Increased ENSO activity coupled with a more southerly located ITCZ during this interval might have led to a weakened summer monsoon and reduced its northward expansion (Koutavas and Lynch-Stieglitz, 2004; Wanner et al., 2008; Böll et al., 2015). Such in-phase behaviour of variability in precipitation patterns and a southerly located ITCZ are observed in data from Lake Malawi, Africa (Konecky et al., 2011), the Tanganyika basin (Tierney et al., 2008), and Tatos basin, Mauritius (de Boer et al., 2014) showing enhanced monsoonal activity and in data from northern and southern Oman and Yemen (Fleitmann et al., 2007) showing weakened monsoon.

Phase V: Climate and vegetation during the period from the Little Ice Age to the present

The cooler and drier Little Ice Age (LIA), prevailing between ~575 to 290 cal yr BP (Paasche and Bakke, 2010; Dixit and Tandon, 2016), reveals changes in precipitation patterns observed in the region (Table 2). During this period, AP was reduced to 74% with low pollen diversity (reduced to 20 species; a decline of 66%). The recorded species with relatively high percentages include *Gluta travancorica*, *Baccaurea courtallensis*, *Scolopia*, *Reinwardtiodendron*, *Syzygium*, *Ixora*, *Turpinia*, and Tiliaceae, along with the appearance of moist deciduous taxa like *Canarium strictum*, *Terminalia*, and *Nothapodytes*. A high percentage of *Rhododendron* and *Impatiens* affirms this cooling phase. High proportions of the pioneer *Artemisia* suggest winter precipitation (Bates et al., 2006) correlating with the LIA (Supplementary Fig. 3). An increased percentage of anthropogenic plant pollen was also encountered in the sediment record. Large numbers of *Acacia* and *Pinus* pollen reflect the advent of human activities for commercial timbering purposes, providing evidence that both climate and human activities are significant drivers in shaping regional vegetation. The greater sand influx above 4 cm is unusual and seems likely to be the result of recent human activities (Fig. 3), including the building of roads and a dam and the clearing of forest for timber, exotic tree plantations, and agriculture. Climatic factors coupled with the advent of anthropogenic activities started the diminishment of shola forest cover (Caner et al., 2007). Overall, the LIA appears to have had a pronounced cool and dry climate (relatively less humid) under the influence of weak monsoonal precipitation, with intensified anthropogenic activities also affecting the environment. Thus, the LIA in the Parsons Valley Lake basin region

https://doi.org/10.1017/qua.2018.58 Published online by Cambridge University Press

appears to suggest a more southerly ITCZ (Haug et al., 2001; Koutavas and Lynch-Stieglitz, 2004; Schneider et al., 2014) coupled with cooler temperatures due to the occurrences of a cluster of solar minima and a high number of strong volcanic events (Wanner et al., 2008; Steinhilber and Beer, 2011; Bradley et al., 2016).

CONCLUSIONS

A 72 cm sediment core collected from the Parsons Valley Lake, Nilgiris, India, covering most of the last 30,000 years was analysed for stable carbon isotopes, geochemistry, sediment texture, and palynological assemblages to gather evidence for the effect of climate change on vegetational succession. The changes in the pattern of vegetation in this region seem to be synchronous with temporal changes in the intensity of the monsoons.

Our multiproxy record shows a regional signal of a warm and wet period at around ~30,000 cal yr BP with the highest AP percentage (81%) and establishment of *Myristica* swamps, which transitions to a cool and dry LGM period with an abundance of temperate taxa. This period was succeeded by a period of fluctuating conditions (~16,300–9,500 cal yr BP) that include an increased importance of C_4 vegetation and an abrupt wet excursion around ~10,700 cal yr BP (interpolated age) associated with the early Holocene intensification of summer monsoons. The early part of the mid-Holocene (~8400 cal yr BP) was characterized by a strengthened monsoon that allowed the shola rainforests to flourish. An environmental threshold around 4800 cal yr BP, marked by an abrupt increase in OM, elevated sand flux, and more negative $\delta^{13}C$, points to a more positive moisture balance. This intense monsoonal trend was interrupted during the late Holocene period by weak and variable summer monsoons associated with strengthened winter monsoons, signifying increased seasonality. This was followed by a cool and dry period interpreted as the LIA. The advent of human activities led to reduced forest cover and the conversion of forest areas into commercial plantations, which is clearly marked in the pollen spectra by the combination of high percentages of *Acacia* and *Pinus* pollen. Thus, it is inferred from the present study that the shola, which has taken several thousands of years to evolve, has decreased considerably through time, as indicated by declining representation of true rainforest elements in the arboreal taxa and replacement of native vegetation with exotic plantation taxa.

SUPPLEMENTARY MATERIAL

To view supplementary material for this article, please visit https://doi.org/10.1017/qua.2018.58

REFERENCES

Allen, K., Dupuy, J.M., Gei, M.G., Hulsho, C., Medvigy, D., Pizano, C., Salgado-Negret, B., et al., 2017. Will seasonally dry tropical forests be sensitive or resistant to future changes in rainfall regimes? *Environmental Research Letters* 12, 023001.

Andreev, A.A., Siegert, C., Klimanov, V.A., Derevyagin, A.Y., Shilova, G.N., Melles, M., 2002. Late Pleistocene and Holocene Vegetation and Climate on the Taymyr Lowland, Northern Siberia. *Quaternary Research* 57, 138–150.

Angeler, D.G., Allen, C.R., 2016. Quantifying resilience. *Journal of Applied Ecology* 53, 617–624.

Ansari, M.H., Vink, A., 2007. Vegetation history and palaeoclimate of the past 30 kyr in Pakistan as inferred from the palynology of continental margin sediments off the Indus Delta. *Review of Palaeobotany and Palynology* 145, 201–216.

Barboni, D., Bonnefille, R., 2001. Precipitation signal in modern pollen rain from tropical forests of southwest India. *Review of Palaeobotany and Palynology* 114, 239–258.

Bard, E., Rostek, F., Turon, J.L., Gendreau, S., 2000. Hydrological impact of Heinrich events in the subtropical northeast Atlantic. *Science* 289, 1321–1324.

Bartlein, P.J., Harrison, S.P., Brewer, S., Connor, S., Davis, B.A.S., Gajewski, K., Guiot, J., et al., 2011. Pollen-based continental climate reconstructions at 6 and 21 ka: a global synthesis. *Climate Dynamics* 37(3–4), 775–802.

Bates, J.D., Svejcar, T., Miller, R.F., Angell, R.A., 2006. The effects of precipitation timing on sagebrush steppe vegetation. *Journal of Arid Environments* 64, 670–697.

Berger, A.L., 1978. Long-term variations of caloric insolation resulting from the Earth's orbital elements. *Quaternary Research* 9, 139–167.

Beuning, K.R.M., Zimmerman, K.A., Ivory, S.J., Cohen, A.S., 2011. Vegetation response to glacial–interglacial climate variability near Lake Malawi in the southern African tropics. *Palaeogeography, Palaeoclimatology, Palaeoecology* 303, 81–92.

Blasco, F., 1971. Montagnes du Sud de l'Inde: forêts, savanes, écologie. *Travaux de la Section scientifique et technique, Institut français de Pondichéry* 10, 436.

Böll, A., Schulz, H., Munz, P., Rixen, T., Gaye, B., Emeis, K.C., 2015. Contrasting sea surface temperature of summer and winter monsoon variability in the northern Arabian Sea over the last 25 ka. *Palaeogeography, Palaeoclimatology, Palaeoecology* 426, 10–21.

Bossuyt, F., Meegaskumbura, M., Beenaerts, M., Gowerdd, J., Pethiyagoda, R., Roelamts, K., Mamaert, A., et al., 2004. Local endemism within the Western Ghat–Sri Lanka biodiversity hotspot. *Science* 306, 479–481.

Bradley, R.S., Wanner, H., Diaz, H.F., 2016). The medieval quiet period. *The Holocene* 26, 990–993. doi: 101177/0959683615622552.

Bunyan, M., Bardhan, S., Jose, S., 2012. The shola (tropical montane forest)-grassland ecosystem mosaic of peninsular India: a review. *American Journal of Plant Sciences* 3, 1632–1639.

Caner, L., Bourgeon, G., 2001. Andisols of the Nilgiris highlands: new insight into their classification, age and genesis. In: Gunell, Y., Radhakrishnan, B.P. (Eds.), *Sahyadri, the Great Escarpment of the Indian Subcontinent (Patterns of Landscape Development in the Western Ghats)*. Geological Society of India, No. 47, pp. 905–918.

Caner, L., Lo Seen, D., Gunnell, Y., Ramesh, B.R., Bourgeon, G., 2007. Spatial heterogeneity of land cover response to climatic change in the Nilgiri highlands (southern India) since the last glacial maximum. *Holocene* 17, 195–205.

Chabangborn, A., Brandefelt, J., Wohlfarth, B., 2013). Asian monsoon climate during the last glacial maximum: palaeo-data–model comparisons. *Boreas* 43, pp 220–242. doi: 10.1111/bor.12032.

Champion, H.G., 1936. A preliminary survey of the forest types of India and Burma. *Indian Forest Records* 1(1), 1–279.

Clark, P.U., Dyke, A.S., Shakun, J.D., Carlson, A.E., Clark, J., Wohlfarth, B., Mitrovica, J.X., Hostetler, S.W., McCabe, A.M., 2009. The last glacial maximum. *Science* 325, 710–714.

Claussen, M., Dallmeyer, A., Bader, J., 2017. Theory and modeling of the African humid period and the green Sahara. *Oxford Research Encyclopedia of Climate Science*. doi: 10.1093/acrefore/9780190228620.013.532.

Cole, L., Bhagwat, S.A., Willis, K.J., 2015. Long-term disturbance dynamics and resilience of tropical peat swamp forests. *Journal of Ecology* 103(1), 16–30.

Corlett, R.T., Primack, R.B., 2006. Tropical rainforests and the need for cross-continental comparisons. *Trends in Ecology and Evolution* 21, 104–110.

Cosford, J., Qing, H., Lin, Y., Eglington, B., Mattey, D., Chen, Y. G., Zhang, M., Cheng, H., 2010. The East Asian monsoon during MIS 2 expressed in a speleothem $\delta^{18}O$ record from Jintanwan Cave, Hunan, China. *Quaternary Research* 73, 541–549.

Davidar, P., Rajagopal, B., Mohandass, D., Puyravaud, J.P., Condit, R., Wright, S.J., Leigh, E.G. Jr., 2007. The effect of climatic gradients, topographic variation and species traits on the beta diversity of rain forest trees. *Global Ecology and Biogeography* 16, pp. 510–518. doi: 10.1111/j.1466-8238.2007.00307.x.

Dean, W.E. Jr., 1974. Determination of carbonate and organic matter in calcareous sediments and sedimentary rocks by loss on ignition: comparison with other methods. *Journal of Sedimentary Petrology* 44, 242–248.

de Boer, E. J., Tjallingii, R., Vélez, M. I., Rijsdijk, K. F., Vlug, A., Reichart, G. J., Hooghiemstra, H., 2014. Climate variability in the SW Indian Ocean from an 8000-yr long multi-proxy record in the Mauritian lowlands shows a middle to late Holocene shift from negative IOD-state to ENSO-state. *Quaternary Science Reviews* 86, 175–189.

Deplazes, G., Luckge, A., Peterson, L.C., Timmermann, A., Hamann, Y., Hughen, K.A., Rohl, U., et al., 2013. Links between tropical rainfall and North Atlantic climate during the last glacial period. *Nature Geoscience* 6, 213–217.

Dixit, Y., Tandon, S.K., 2016. Hydroclimatic variability on the Indian subcontinent in the past millennium: review and assessment. *Earth-Science Reviews* 161, 1–15.

Dutt, S., Gupta, A.K., Clemens, S.C., Cheng, H., Singh, R.K., Kathayat, G, Edwards, R.L., 2015. Abrupt changes in Indian summer monsoon strength during 33,800 to 5500 years B.P. *Geophysical Research Letters* 42, 5526–5532.

Erdtrnan, G., 1943. *An Introduction to Pollen Analysis*. Chronica Botanica Company, Waltham, pp. 1–239.

Farooqui, A., Pattan, A., Parthiban, J.N., Srivastava, J., Ranjana, 2014. Palynological record of tropical rainforest vegetation and sea level fluctuations since 140 Ka from sediment core, south-eastern Arabian Sea. *Palaeogeography, Palaeoclimatology, Palaeoecology* 411, 95–109.

Farooqui, A., Ray, J.G., Farooqui, S.A., Tiwari, R.K., Khan, Z.A., 2010. Tropical rainforest vegetation, climate and sea level during the Pleistocene in Kerala, India. *Quaternary International* 213, 2–11.

Farrera, I., Harrison, S.P., Prentice, I.C., Ramstein, G., Guiot, J., Bartlein, P.J., Bonnefille, R., et al., 1999. Tropical climates at the last glacial maximum: a new synthesis of terrestrial palaeoclimate data. I. Vegetation, lake levels and geochemistry. *Climate Dynamics* 15, 823–856.

Feeley, K.J., Wright, S.J., Supardi, M.N.N., Kassim, A.R., Davies, S.J., 2007. Decelerating growth in tropical forest trees. *Ecology Letters* 10, 461–469.

Fleitmann, D., Burns, S.J., Mangini, A., Mudelsee, M., Kramers, J., Villa, I., et al., 2007. Holocene ITCZ and Indian monsoon dynamics recorded in stalagmites from Oman and Yemen (Socotra). *Quaternary Science Reviews* 26, 170–188.

Fleitmann, D., Burns, S.J., Neff, U., Mudelsee, M., Mangini, A., Kramers, J., Matter, A., 2004. Holocene records of rainfall variation and associated ITCZ migration from stalagmites from northern and southern Oman. In: Diaz, H.F., Bradley, R.S. (Eds.), *The Hadley Circulation: Present, Past, and Future*. Advances in Global Change Research Vol. 21. Springer, Dordrecht, pp. 259–287.

Fleitmann, D., Burns, S. J., Pekala, M., Mangini, A., Al-Subbary, A., Al-Aowah, M., Kramers, J., Matter, A., 2011. Holocene and Pleistocene pluvial periods in Yemen, southern Arabia. *Quaternary Science Reviews* 30, 783–787.

Gadgil, S., 2003. The Indian monsoon and its variability. *Annual Reviews of Earth and Planetary Science* 31, 429–467.

Galy, V., François, L., France-Lanord, C., Faure, P., Kudrass, H., Palhol, F., Singh, S., 2008. C4 plants decline in the Himalayan basin since the Last Glacial Maximum. *Quaternary Science Reviews* 27, 1396–1409.

Ghate, U., Joshi, N.V., Gadgil, M., 1998. On the patterns of tree diversity in the Western Ghats of India. *Current Science* 75, 594–603.

Grimm, E.C., 2011. Tilia. Version 1.7.16 [computer software]. Illinois State Museum, Research and Collections Center, Springfield, Ill.

Gupta, A., Anderson, D.M., Overpeck, J.T., 2003. Abrupt changes in the Asian southwest monsoon during the Holocene and their links to the North Atlantic Ocean. *Nature* 421, 354–357.

Hamdan, M.A., Brook, G.A., 2015. Timing and characteristics of Late Pleistocene and Holocene wetter periods in the Eastern Desert and Sinai of Egypt, based on ^{14}C dating and stable isotope analysis of spring tufa deposits. *Quaternary Science Reviews* 130, 168–188.

Haug, G.H., Hughen, K.A., Sigman, D.M., Peterson, L.C., Röhl, U., 2001. Southward migration of the Intertropical Convergence Zone through the Holocene. *Science* 293, 1304–1308.

Holmes, J., Hoelzmann, P., 2017. The late Pleistocene–Holocene African humid period as evident in lakes. *Oxford Research Encyclopedia of Climate Science*. doi: 10.1093/acrefore/9780190228620.013.531.

Jacobson, G.L., Grimm, E.C., 1986. A numerical analysis of Holocene forest and prairie vegetation in central Minnesota. *Ecology* 67, 958–966.

Jose, F.C., 2012. The "living fossil" shola plant community is under threat in upper Nilgiris. *Current Science* 102, 1091–1092.

Karunakaran, P.V., Rawat, G.S., Uniyal, V.K., 1998. *Ecology and Conservation of the Grasslands of Eravikulam National Park, Western Ghats*. Wildlife Institute of India, Dehra Dun, India.

Konecky, L., Russell, J, M., Johnson, T.C., Brown, E.T., Berke, M.A., Werne, J.P., Huang, Y., 2011. Atmospheric circulation patterns during late Pleistocene climate changes at Lake Malawi, Africa Bronwen. *Earth and Planetary Science Letters* 312, 318–326.

Koutavas, A., Lynch-Stieglitz, J., 2004. In: Diaz, H.F., Bradley, R.S. (Eds.), *The Hadley Circulation: Present, Past, and Future*. Advances in Global Change Research Vol. 21. Springer, Dordrecht, pp. 347–369.

Kristen, I., Fuhrmann, A., Thorpe, J., Röhl, U., Wilkes, H., Oberhänsli, H., 2007. Hydrological changes in southern Africa over the last 200 Ka as recorded in lake sediments from the Tswaing impact crater. *South African Journal of Geology* 110(2–3), 311–326.

Krumbein, W.C., Pettijohn, F.J., 1938. *Manual of Sedimentary Petrography*. Appleton Century-Crofts, New York, pp. 230–233.

Kumar, P., Pattanaik, J.K., Ojha, S., Gargari, S., Joshi, R., Chopra, S., Kanjilal, D., 2015. A new AMS facility at Inter-University Accelerator Centre, New Delhi. *Nuclear Instruments and Methods in Physics Research Section B* 361, 115–119.

Kumaran, K.P.N., Limaye, R.B., Nair, K.M., Padmalal, D., 2008. Palaeoecological and palaeoclimate potential of subsurface palynological data from the Late Quaternary sediments of South Kerala Sedimentary Basin, southwest India. *Current Science* 95, 515–526.

Kutzbach, J.E., Guetter, P., 1986. The influence of changing orbital parameters and surface boundary conditions on climate simulations for the past 18 000 years. *Journal of the Atmospheric Sciences* 43, 1726–1759.

Liu, X., Liu, Z., Kutzbach, J.E., Clemens, S.C., Prell, W.L., 2006. Hemispheric insolation forcing of the Indian Ocean and Asian Monsoon: local versus remote impacts. *Journal of Climate* 19, 6195–6208.

Liu, Z.T., Colin, C., Trentesaux, A., Siani, G., Frank, N., Blamart, D., Farid, S., 2005. Late Quaternary climatic control on erosion and weathering in the eastern Tibetan Plateau and the Mekong Basin. *Quaternary Resources* 63, 316–328.

Markgraf, V., Whitlock, C., Haberle, S., 2007. Vegetation and fire history during the last 18,000 cal yr B.P. in Southern Patagonia: Mallín Pollux, Coyhaique, Province Aisén (45°41′30″ S, 71°50′ 30″ W, 640 m elevation). *Palaeogeography, Palaeoclimatology, Palaeoecology* 254, 492–507.

Mathur, H.N., Francis, H., Raj, S.F.H., Naithan, S., 1984. Ground water quality (pH) under different vegetative covers at Osamund (Nilgiri Hills). *Indian Forester* 10, 110–115.

Meir, P., Wood, T.E., Galbraith, D.R., Brando, P.M., Da Costa, A. C.L., Rowland, L., Ferreira, L.V., 2015. Threshold responses to soil moisture deficit by trees and soil in tropical rain forests: insights from field experiments. *BioScience* 65, 882–892.

Mitchum, R.M. Jr., 1977. Seismic Stratigraphy and Global Changes of Sea Level: Part 11. Glossary of Terms used in Seismic Stratigraphy: Section 2. Application of Seismic Reflection Configuration to Stratigraphic Interpretation, AAPG Memoir, 205–212.

Moore, P.D., Webb, J.A., Collinson, M.E., 1991. *Pollen Analysis*. 2nd ed. Blackwell Scientific, Oxford.

Moy, C.M., Seltzer, G.O., Rodbell, D.T., Anderson, D.M., 2002. Variability of El Niño/Southern Oscillation activity at millennial timescales during the Holocene epoch. *Nature* 420, 162–165.

Myers, N., Mittermeier, R.A., Mittermeier, C.G., da Fonseca, G.A. B., Kent, J., 2000. Biodiversity hotspots for conservation priorities. *Nature* 403, 853–858.

Naqvi, S.M., Rogers, J.W., 1987. *Precambrian Geology of India*. Clarendon Press, Oxford.

Newnham, R.M., Lowe, D.J., Giles, T., Alloway, B.V., 2007. Vegetation and climate of Auckland, New Zealand, since ca. 32 000 cal. yr ago: support for an extended LGM. *Journal of Quaternary Science* 22, 517–534.

Overpeck, J., Anderson, D., Trumbore, S., Prell, W., 1996. The southwest Indian Monsoon over the last 18000 years. *Climate Dynamics* 12, 213–215.

Overpeck, J.T., 1993. The role and response of continental vegetation in the global climate system. In: Eddy, J.A., Oeschger, H. (Eds.), *Global Changes in the Perspective of the Past*. Wiley, New York, pp. 221–237.

Paasche, Ø., Bakke, J., 2010. Defining the Little Ice Age. *Climate of the Past Discussion* 6, 2159–2175.

Peterson, L.C., Haug, G.H., 2006. Variability in the mean latitude of the Atlantic Intertropical Convergence Zone as recorded by riverine input of sediments to the Cariaco basin (Venezuela). *Palaeogeography, Palaeoclimatology, Palaeoecology* 3, 97–113.

Plater, J., Boyle, J.F., Mayers, C., Turner, S.D., Stroud, R.W., 2006. Climate and human impact on lowland lake sedimentation in Central Coastal California: the record from c. 650 AD to the present. *Regional Environmental Change* 6, 71–85.

Power, M.J, Whitlock, C., Bartlein, P., Stevens, L.R., 2006. Fire and vegetation history during the last 3800 years in northwestern Montana. *Geomorphology* 75, 420–436.

Pramod, P., Daniels, R.J.R., Joshi, N.V., Gadgil, M., 1997. Evaluating bird communities of Western Ghats to plan for a biodiversity friendly development. *Current Science* 73, 156–162.

Prasad, V., Farooqui, A., Tripathi, S.K.M., Garg, R., Thakur, B., 2009. Evidence of late Palaeocene–early Eocene equatorial rain forest refugia in southern western Ghats, India. *Journal of Biosciences* 34, 777–797.

Priyanka, R., Achyuthan, H., Geethanjali, K., Kumar, P., Chopra, S., 2018. Late Pleistocene paleoflood deposits identified by grain size signatures, Parsons Valley Lake, Nilgiris, Tamil Nadu. *Journal of Geological Society of India* 91, pp. 517–644.

Rajagopalan, G., Sukumar, R., Ramesh, R., 1997. Late Quaternary vegetational and climatic changes from tropical peats in southern India, an extended record up to 40,000 years BP. *Current Science* 73, 60–63.

Ramisch, A., Lockot, G., Haberzettl, T., Hartmann, K., Kuhn, G., Lehmkuhl, F., Schimpf, S., et al., 2016. A persistent northern boundary of Indian summer monsoon precipitation over Central Asia during the Holocene. *Scientific Reports* 6, 25791.

Roy, P.D., Singhvi, A.K., 2016. Climate variation in the Thar Desert since the last glacial maximum and evaluation of the Indian monsoon. *Revista Especializada en Ciencias Químico-Biológicas* 19, 32–44.

Ruiz-Zapata, B., Gil-García, M.J., Bustamante, I., 2010. Paleoenvironmental reconstruction of Las Tablas de Daimiel and its evolution during the Quaternary period. In: Sanchez-Carrillo, S., Angeler, D.G. (Eds.), *Long-Term Research in Las Tablas de Daimiel*. Springer, Dordrecht. pp. 23–43.

Russella, J.M., Vogel, H., Konecky, B.L., Bijaksana, S., Huang, Y., Melles, M., Wattrus, N., Costa, K., King, J.W., 2014. Glacial forcing of central Indonesian hydroclimate since 60,000 y B.P. *Proceedings of the National Academy of Sciences USA* 111, 5100–5105.

Sadler, P. M., 1999. The influence of hiatuses on sediment accumulation rates. *GeoResearch Forum* 5, 15–40.

Schneider, T., Bischoff, T., Haug, G.H., 2014. Migrations and dynamics of the intertropical convergence zone. *Nature* 513, 45–53.

Servant-Vildary, S., Servant, M., Jimenez, O., 2001. Holocene hydrological and climatic changes in the southern Bolivian Altiplano according to diatom assemblages in paleowetlands. *Hydrobiologica* 466, 267–277.

Shin, S.I., Liu, Z., Otto-Bliesner, B.L., Brady, E.C., Kutzbach, J.E., Harrison, S.P., 2003. A simulation of the last glacial maximum climate using the NCAR CSM. *Climate Dynamics* 20, 127–151.

Sinninghe Damsté, J.P., Verschuren, D., Ossebaar, J., Blokker, J., Houten, R., van der Meer, M.T.J., Plessen, B., Schouten, S., 2011. A 25,000-year record of climate-induced changes in lowland vegetation of eastern equatorial Africa revealed by the stable carbon-isotopic composition of fossil plant leaf waxes. *Earth and Planetary Science Letters* 302, 236–246.

Sirocko, F., Sarnthein, M., Erlenkeuser, H., Lange, H., Arnold, M., Duplessy, J.C., 1993. Century scale events in monsoon climate over the past 24,000 years. *Nature* 364, 322–324.

https://doi.org/10.1017/qua.2018.58 Published online by Cambridge University Press

Steinhilber, F., Beer, J., 2011. Solar activity—the past 1200 years. *PAGES News* 19(1), 5–6.

Steinke, S., Mohtadi, M., Prange, M., Varma, V., Pittauerova, D., Fischer, H.W., 2014. Mid- to late-Holocene Australian–Indonesian summer monsoon variability. *Quaternary Science Reviews* 93, 142–154.

Sukumar, R., Ramesh, R., Pant, R.K., Rajagopalan, G., 1993. A $\delta^{13}C$ record of late Quaternary climate change from tropical peats in southern India. *Nature* 364, 703–706.

Suryaprakash, I., 1999. Plant Communities in the Montane Region of Nilgiris, Southern India: Analysis of Present and Past Vegetation Based on Plant-Pollen Assemblages. PhD thesis, Sallm Ali School of Ecology and Environmental Sciences, Pondicherry University, Pondicherry, India.

Swarupanandan, K., Sasidharan, N., Chacko, K.C., Basha, S.C., 1998. *Studies on the Shola Forest of Kerala*. Kerala Forest Research Institute Research Report 158. Kerala Forest Research Institute, Peechi, India.

Thevenon, F., Adatte, T., Spangenberg, J.E., Anselmetti, F.S., 2012. Elemental (C/N ratios) and isotopic ($\delta 15N_{org}$, $\delta 13C_{org}$) compositions of sedimentary organic matter from a high-altitude mountain lake (Meidsee, 2661 m a.s.l., Switzerland): implications for late glacial and Holocene Alpine landscape evolution. *The Holocene* 22, 1135–1142.

Thomas, S.M., Palmer, M.W., 2007. The montane grasslands of the Western Ghats, India: community ecology and conservation. *Community Ecology* 8, 67–73.

Tierney, J.E., Russell, J.M., Huang, Y., Jaap, S., Damsté, S., Hopmans, E.C., Cohen, A.S., 2008. Northern Hemisphere controls on tropical Southeast African climate during the past 60,000. *Science* 322, 252–255.

Tiwari, M., Ramesh, R., Somayajulu, B.K.L., Jull, A.J.T., Burr, S.G., 2006. Paleomonsoon precipitation deduced from a sediment core from the equatorial Indian Ocean. *Geo-Marine Letters* 26, 23–30.

Usoskin, I.G., Solanki, S.K., Kovalstov, G.A., 2007. Grand minima and maxima of solar activity: new observational constraints. *Astronomy & Astrophysics* 471, 301–309.

Vasanthy, G., 1988. Pollen analysis of late Quaternary sediments: evolution of upland savanna in Sandynallah (Nilgiris, south India). *Review of Palaeobotany and Palynology* 55, 175–192.

Vishnu-Mittre, Gupta, H.P., 1968. A living fossil plant community in South Indian hills. *Current Science* 37, 671–672.

Wacker, L., Nemec, M., Bourquin, J., 2010. A revolutionary graphitisation system: fully automated, compact and simple. *Nuclear Instruments and Methods in Physics Research B* 268(7–8), 931–934.

Walker, M., Johnsen, S., Rasmussen, S.O., Popp, T., Steffensen, J.P., Gibbard, P., Hoek, W., et al., 2009. Formal definition and dating of the GSSP (Global Stratotype Section and Point) for the base of the Holocene using the Greenland NGRIP ice core, and selected auxiliary records. *Journal of Quaternary Science* 24, 3–17.

Wang, L.J., Sarnthein, M., Erlenkeuser, H., Grimalt, J.O., Grootes, P.M., Heilig, S., Ivanova, E.V., Kienast, M., Pelejero, C., Pflaumann, U., 1999. East Asian monsoon climate during the late Pleistocene: high-resolution sediment records from the South China Sea. *Marine Geology* 156, 245–284.

Wang, Y., Liu, X., Herzschuh, U., 2010. Asynchronous evolution of the Indian and East Asian Summer monsoon indicated by Holocene moisture patterns in monsoonal central Asia. *Earth-Science Reviews* 103, 135–153.

Wanner, H., Beer, J., Bütikofer, J., Crowley, T.J., Cubasch, U., Flückiger, J., Goosse, H., et al., 2008. Mid- to late Holocene climate change: an overview. *Quaternary Science Reviews* 27, 1791–1828.

Yancheva, G., Nowaczyk, N.R., Mingram, J., Dulski, P., Schettler, G., Negendank, J.F.W., Liu, J., Sigman, D.M., Peterson, L.C., Haug, G.H., 2007. Influence of the Intertropical convergence zone on the East Asian monsoon. *Nature* 445, 74–77.

Yu, G., Xue, B., Wang, S., Liu, J., 2000. Lake records and LGM climate in China. *Chinese Science Bulletin* 45, 1158–1164.

Zhang, W., Ming, Q., Shi, Z., Chen, G., Niu, J., Lei, G., Chang, F., Zhang, H., 2014. Lake sediment records on climate change and human activities in the Xingyun Lake catchment, SW China. *PLoS ONE* 9(7 doi: 10.1371/journal.pone.0102167

Zhong, W., Xue, J., Zheng, Y., Ma, Q., Cai, Y., Ouyang, J., Cao, J., Tang, X., 2012. Sediment geochemistry of Dahu Swamp in the Nanling Mountains, South China: implication for catchment weathering during the last 16,000 years. *International Journal of Earth Science* 101, 453–462.